

# DIRECTIONALLY-SOLIDIFIED Co-Co<sub>7</sub>W<sub>6</sub> EUTECTIC COMPOSITES FOR TURBINE BLADES

Mohamed A. Taha<sup>x</sup>

## ABSTRACT

Structural changes that arise due to growth rate variations in Co-Co<sub>7</sub>W<sub>6</sub> directionally solidified eutectic composites have been observed. The growth rates (R) considered ranged from 1.38 to 55.5  $\mu\text{m/s}$ . The temperature gradient was kept constant at an average value of  $13 \pm 1$  K/mm. The as-solidified structure, which is produced by quenching from above the peritectoid temperature changes greatly with R. At low R, aligned lamellar morphology is observed. The increase in R gradually causes perforations, breaking into short ribbon-shape with width to thickness ratio decreasing with increasing R. Further increase in R causes first longitudinal branching in the ribbon plane, then the appearance of short side branches. At R = 55.5  $\mu\text{m/s}$  the structure is cellular, each cell consisting of a single dendrite-like Co-Co<sub>7</sub>W<sub>6</sub> phase. In spite of these variations in structure, the interlamellar or "inter-ribbon" spacing was found to obey the relationship  $\bar{\lambda} = nR^{-0.5}$ . Further observations show the presence of faults in the steady-state grown structure. The peritectoid transformation which occurs in the Co matrix has no influence on the shape and dimensions of the Co<sub>7</sub>W<sub>6</sub> phase. The addition of small solute elements of C, Al and Cr promotes the cellular morphology both at high and low R.

## INTRODUCTION

Attention has been focused on the directional solidification of high temperature eutectic alloys to provide composite materials for future advanced turbine engines. It has been widely demonstrated that these composites possess very attractive properties. In this regard, a number of studies have been made to develop high temperature nickel and cobalt base composites using directional solidification. Regarding cobalt, which has increasing availability and reasonable price, its alloys have aided the solution of problems involving thermal barriers as well as elevated temperature corrosion and wear resistance for various types of prime movers. Indeed expanding usage of cobalt alloys is expected and they should continue to serve in meeting tough

---

<sup>x</sup> Professor, Department of Design and Production Engineering, Faculty of Engineering, Ain-Shams University, Abbaseia, Cairo - EGYPT.

engineering requirements. One of the high temperature cobalt base eutectics is the Co-W alloy. Literature survey shows that only very few information are present on its microstructure. In the present paper a description of the microstructures obtained by directional solidification of the eutectic is given.

### EXPERIMENTAL PROCEDURE

#### Material Used

The Co-W eutectic alloys used in the present work were prepared in a vacuum induction furnace using high purity electrolytic cobalt and tungsten metals. In a preliminary investigation a series of experiments consisting of alloy preparation, directional solidification at a growth rate of  $16.6 \mu\text{m/s}$  and a temperature gradient of  $13\text{K/mm}$  then microstructure observations, the eutectic composition was found to be at 44.5 wt% W. In literature, it is reported that the eutectic occurs at 45 wt% W (1,2). The melting point was determined by differential thermal analysis and was found to be 1743 K while previous were show values of 1753 K (1) and 1738 K (2). Generally, after preparing the alloys, they have been cast in ceramic moulds to form rods which were then slightly turned and used for directional solidification experiments.

Another group of eutectic alloys with similar W content have been prepared to which different slight additions of solute elements were added, as given in TABLE 1. In all cases the elements added were with high purity.

TABLE 1 - Composition of the alloys( wt% )

Alloy	Co	W	C	Al	Cr
Pure eutectic	bal.	44.5	-	-	-
Eutectic with C addition	bal.	44.5	0.1	-	-
	bal.	44.5	0.2	-	-
Eutectic with Al addition	bal.	44.5	-	0.1	-
	bal.	44.5	-	0.3	-
Eutectic with Cr addition	bal.	44.5	-	-	0.1
	bal.	44.5	-	-	0.3

#### Unidirectional Solidification

Steady state unidirectional solidification was applied on the present eutectic alloys. In the apparatus used the specimen, 14 mm diameter and 170 mm long, is inserted in an alumina tube and withdrawn downwards from a high temperature Tamman furnace through a water cooling head at a constant rate (growth rate, R). R was varied between 1.38 and  $55.5 \mu\text{m/s}$ . The temperature gradient (G) was kept approximately constant in the different experiments by slight regulation of the furnace temperature, where an average value of  $13 \pm 1 \text{ K/mm}$  was achieved.

## RESULTS AND DISCUSSION

Specimens completely directionally solidified showed structure in which the matrix has been subjected to peritectoid transformation. Therefore, specimens were quenched after directional solidification of a certain length and a zone of about 20 mm long at the terminal of this length is quenched from above the peritectoid temperature i.e 1373 K. In this zone, the as-solidified structure is present and observed.

### As-Solidified Structure

Different eutectic morphologies are observed with increasing the growth rate  $R$  from 1.38 to 55.5  $\mu\text{m/s}$  and keeping temperature gradient  $G$  at approximately constant value of  $13 \pm 1 \text{ K/mm}$ . These different morphologies are shown by optical microscopy in Fig.1 and by electron scanning microscopy in Fig.2. At low  $R$  of 1.38  $\mu\text{m/s}$ , the  $\text{Co}_7\text{W}_6$  phase appears to solidify in the form of aligned lamellae, Fig.1(a), but from the electron scanning micrograph, Fig.2(a), it is apparent that these lamellae are actually long and wide ribbons. With increasing  $R$  the lamellae (or wide ribbons) gradually become broken and less perfect with increasing number of protuberances and perforations. The ribbon shape is more clear and their width to thickness ratio decreases to such an extent that at low magnifications and in two dimensions, some of them appear as fibres, Fig.1(b) and 2(b). This structure is observed in some grains at  $R$  of 4.2  $\mu\text{m/s}$ , while other grains still exhibit the so-called aligned lamellae. Above  $R$  of 4.2  $\mu\text{m/s}$ , most grains in the specimen exhibited this type of ribbon structure. Further increase in  $R$  causes gradual branching of the  $\text{Co}_7\text{W}_6$  phase, in the ribbon plane, in the form of longitudinal or short side branching as observed at  $R=8.3$  and 16.6  $\mu\text{m/s}$ , Fig.1(c). The detailed study with electron scanning microscope shows that the highly faulted ribbons break down into bundles of fibres, Fig.2(c), which then continue to grow separately as observed in some grains of the specimen, Fig.2(d), but still possessing the faceted cross-section. These fibres are in fact finely divided ribbons, and previous work (3,4) on other systems have shown that such "ribbon-fibre" transition is one of scale rather than type, based on their observations that the orientation relationships are similar in both structures. Short side branches are also observed to form at the same time from the ribbons and fibres, Fig.1(c) and 2(e). By increasing  $R$  above 16.6  $\mu\text{m/s}$  cellular-like morphology is observed in some grains. Some of the cells exhibit a single  $\text{Co}_7\text{W}_6$  ribbon or fibre with long side branches. Some others exhibit short broken ribbon-like morphology with coarse or depleted  $\text{Co}_7\text{W}_6$  cell boundaries. At  $R=55.5 \mu\text{m/s}$  the structure is completely cellular, as shown in Fig.1(d). In all cases, it is observed that more than one type of structure can form simultaneously. In completely directionally solidified specimens, the cellular morphology is always observed at the top of the specimens. These types of structures, observed here excluding side branching, are similar to that previously observed in  $\text{Al-Al}_9\text{Co}_2$

directionally solidified eutectic( 5 ). Moreover, the broken lamellar morphology has been observed in those systems which have a low volume fraction of a phase ( $V_f$ ) with a large entropy of solution ( $\Delta S_\alpha$ ).(6,7,8,9,10). Examples include in addition

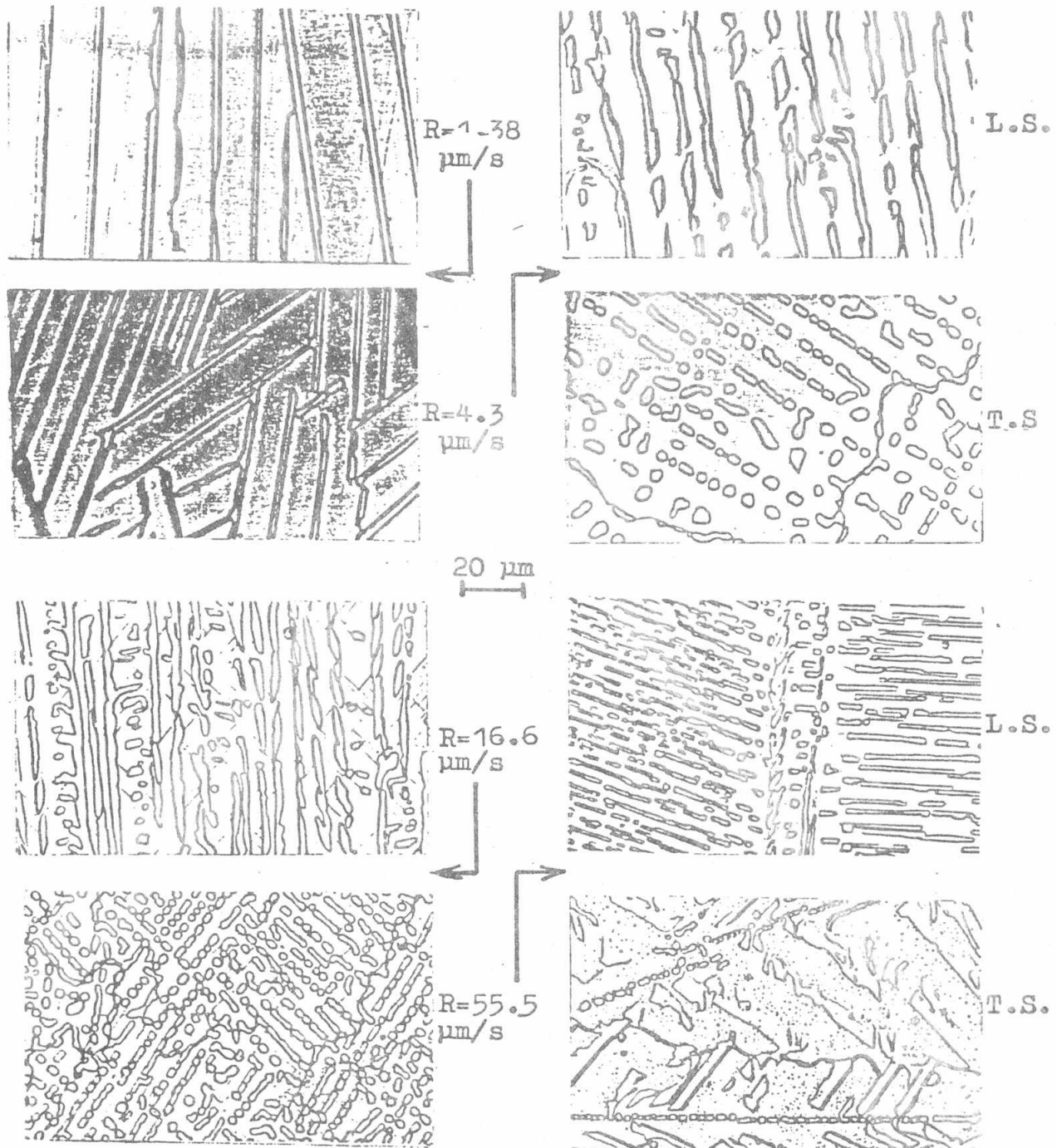


Fig.1: Optical micrographs showing longitudinal(L.S.) and transverse(T.S.) sections indicating structures observed in unidirectionally-solidified eutectic at different  $R$  and constant  $G$  of  $13 \pm 1 \text{ K/mm}$ .



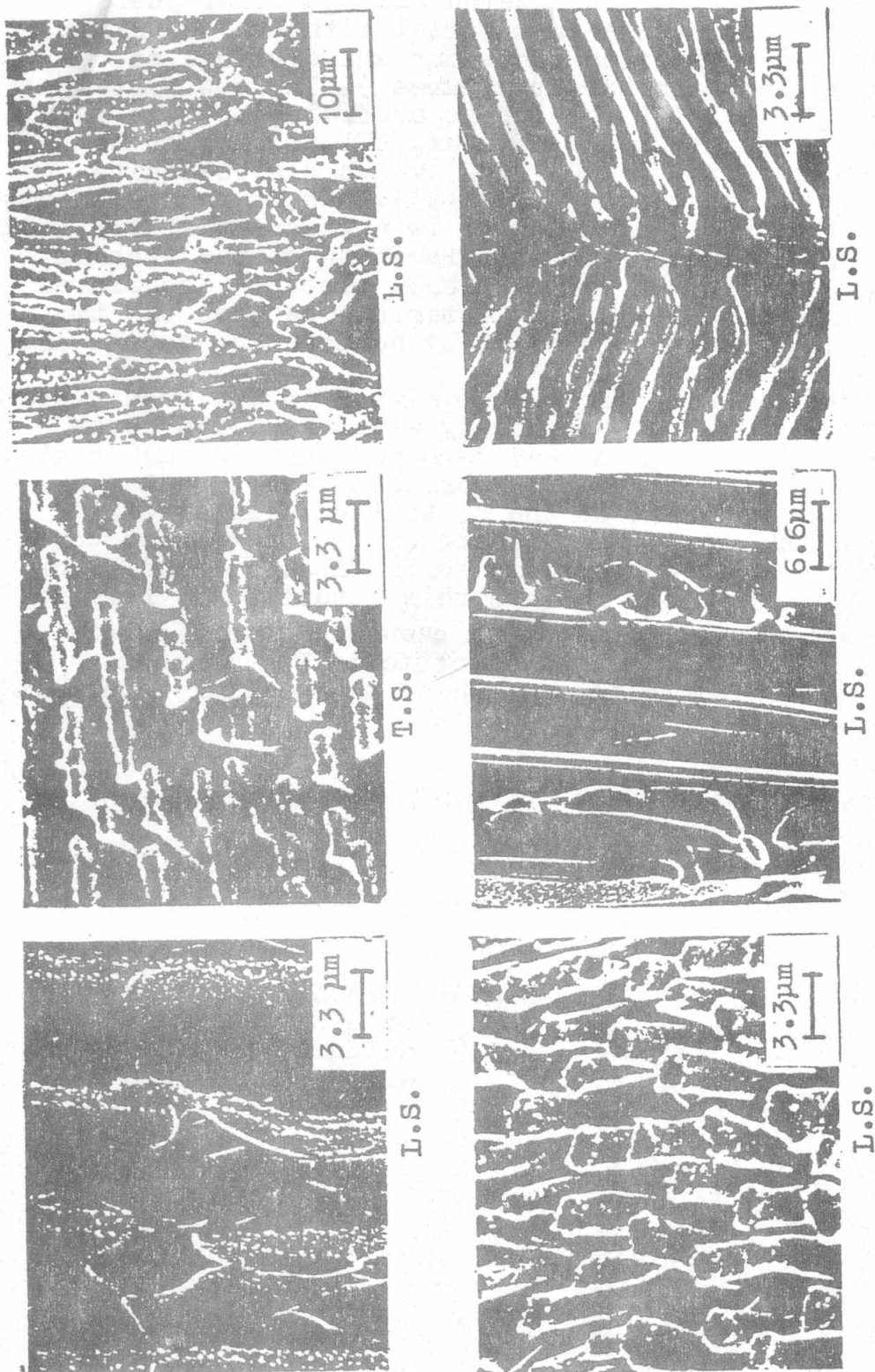


Fig.2: Scanning electron micrographs showing longitudinal-sections(L.S.) and transverse-sections(T.S.) indicating:  
 (a) non-perfect lamellae, (b) ribbons, (c) longitudinal branching, (d) rods, (e) short side-branching and (f) cell in which long side branched phase is observed. The structures are observed with increasing R gradually from 1.38 to 55.5  $\mu\text{m/s}$ .

to the Al-Al<sub>9</sub>Co<sub>2</sub> system(5) the Al-Al<sub>3</sub>Ni, Pb-Ag, Sn-Zn, Bi-Ag (6,7,8), Al-Al<sub>3</sub>Fe(11) and Bi-Zn(12) systems. In these systems, where the matrix solidifies non-faceted and the minor phase tends to facets, the structure is abnormal with  $\Delta S_{\alpha} \approx 23 \text{ J/mol./K}$  ( this value indicates faceting behaviour and distinguish between the normal and abnormal structures ). In Co-W system Co<sub>7</sub>W<sub>6</sub> phase has  $V_f = 0.23(12)$ , which is according to this rule, is not small enough for such a behaviour, but is similar to that in Bi-Au system with  $V_f = 0.22(12)$  which also exhibits a broken lamellar or ribbon morphology(13). Thus it seems, as also already reported(14,15), that a low  $V_f$  is not essential for such structure to form. In these systems, branching of the ribbons occurs frequently within the ribbon plane, probably associated with the resistance of a low energy interface between the two phases in order to overcome occlusion by nonfaceting matrix and to maintain physical continuity(11).

Further structural changes observed at high R in the co-W system is the formation of cellular morphology with the Co<sub>7</sub>W<sub>6</sub> phase with long side branches. It has been reported that in such systems under consideration, growth restrictions can lead to a large compositional boundary layer at the solid/liquid interface that can promote constitutional undercooling with respect to the faceting phase under appropriate solidification conditions. In this case, the system can relieve this situation by forming a faceted cellular interface (11). The quenched interface of directionally solidified Co-Co<sub>7</sub>W<sub>6</sub> eutectic in Fig.3 shows a well-developed cell growing in advance of the general interface.

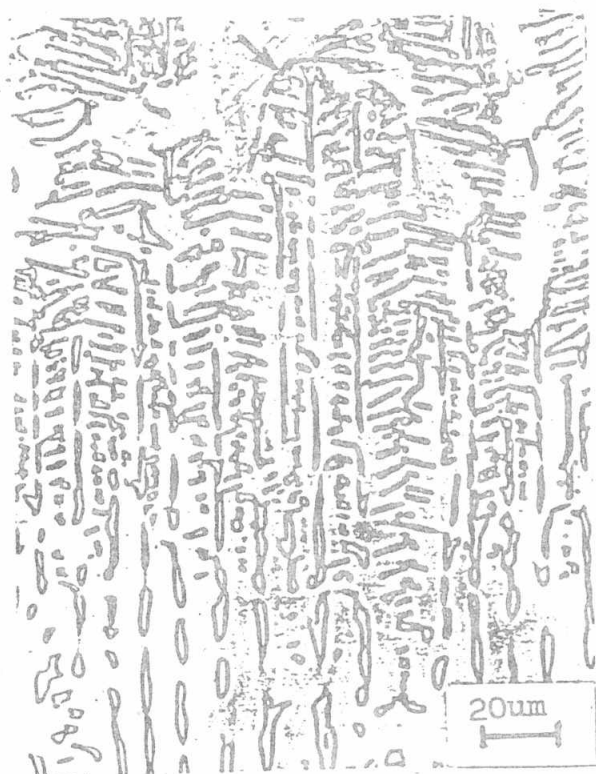


Fig.3: Quenched interface of a directionally solidified Co-Co<sub>7</sub>W<sub>6</sub> alloy at  $R=4.2 \mu\text{m/s}$ .

### Interlamellar (or inter-ribbon) spacing

Interlamellar or inter-ribbon spacing was measured on transverse sections of specimen parts quenched from above the peritectoid temperature. At low R it was easy to find perfect lamellae for measurement. At higher R where the morphology changes to ribbon and then is divided into nearly rod-like shape, care was taken to make the measurements between the centrelines of the main ribbon planes as shown in Fig.4. At much higher R where the cellular morphology is the most frequent, it was possible by taking many transverse sections from the specimen to find out some grains in which ribbons are present in the cell centre. Due to fluctuations in structure in the same specimen, an average value of inter-ribbon spacing  $\bar{\lambda}$  is calculated. Fig.5 shows a log-log representation of  $\bar{\lambda}$  vs. R. The well known relationship

$$\bar{\lambda} = nR^{-0.5}$$

was found to be obeyed over the range of R used. It is clear that values of  $\bar{\lambda}$  measured in specimens even containing finely divided ribbons (rod-like) or cellular morphology also obeyed the above relationship. A similar conclusion has been also reported on the Al-Al<sub>9</sub>Co<sub>2</sub> eutectic(5).

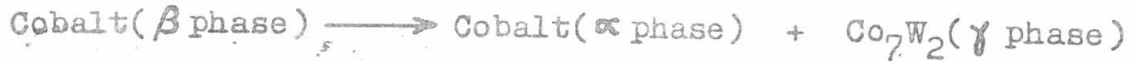
### Structural faults

In addition to the above structural features, specimens grown under steady state conditions, show some faults in the structure. Examples of these faults are shown in Fig.6. The scanning electron micrograph in Fig.6(a), shows longitudinal branching then rewelding of Co<sub>7</sub>W<sub>6</sub> ribbons or fibres. In Fig.6(b), fluctuations in rod diameter which can lead to its termination is observed for Co<sub>7</sub>W<sub>6</sub> phase. In Fig.6(c), banding defect is observed where a completely Co<sub>7</sub>W<sub>6</sub> depleted zone is clear, above which new nucleation of Co<sub>7</sub>W<sub>6</sub> lamellae starts to occur then growth continue as broken lamellae or ribbons in the axial direction. In the present eutectic faults may always arise since the structure is very sensitive to solidification conditions.

### Structure With Peritectoid Transformation

Another microstructural condition in which the eutectic was examined is that with peritectoid transformation. This structure is produced in the specimens, during the directional solidification experiment, if they are withdrawn below the peritectoid temperature. At all R employed the Co<sub>7</sub>W<sub>6</sub> phase already formed in the solidification stage did not change where same shape and spacing remained. Fig.7 shows a scanning electron micrograph of the structure obtained, where the matrix is consisting of two phases. The available information on the system(1,2) indicate that in the Co-W system, the peritectoid

transformation occurs where the cobalt ( $\beta$  phase) decomposes according to the equation:



By deep etching the cobalt ( $\alpha$  phase) is attacked and plate-like  $\text{Co}_7\text{W}_2$  phase appears in the micrograph, Fig.7.

Fig.4:  $\bar{\lambda}$  measurements:  
(a) at low R,  
interlamellar and  
(b) at high R,  
inter-ribbon  
spacings

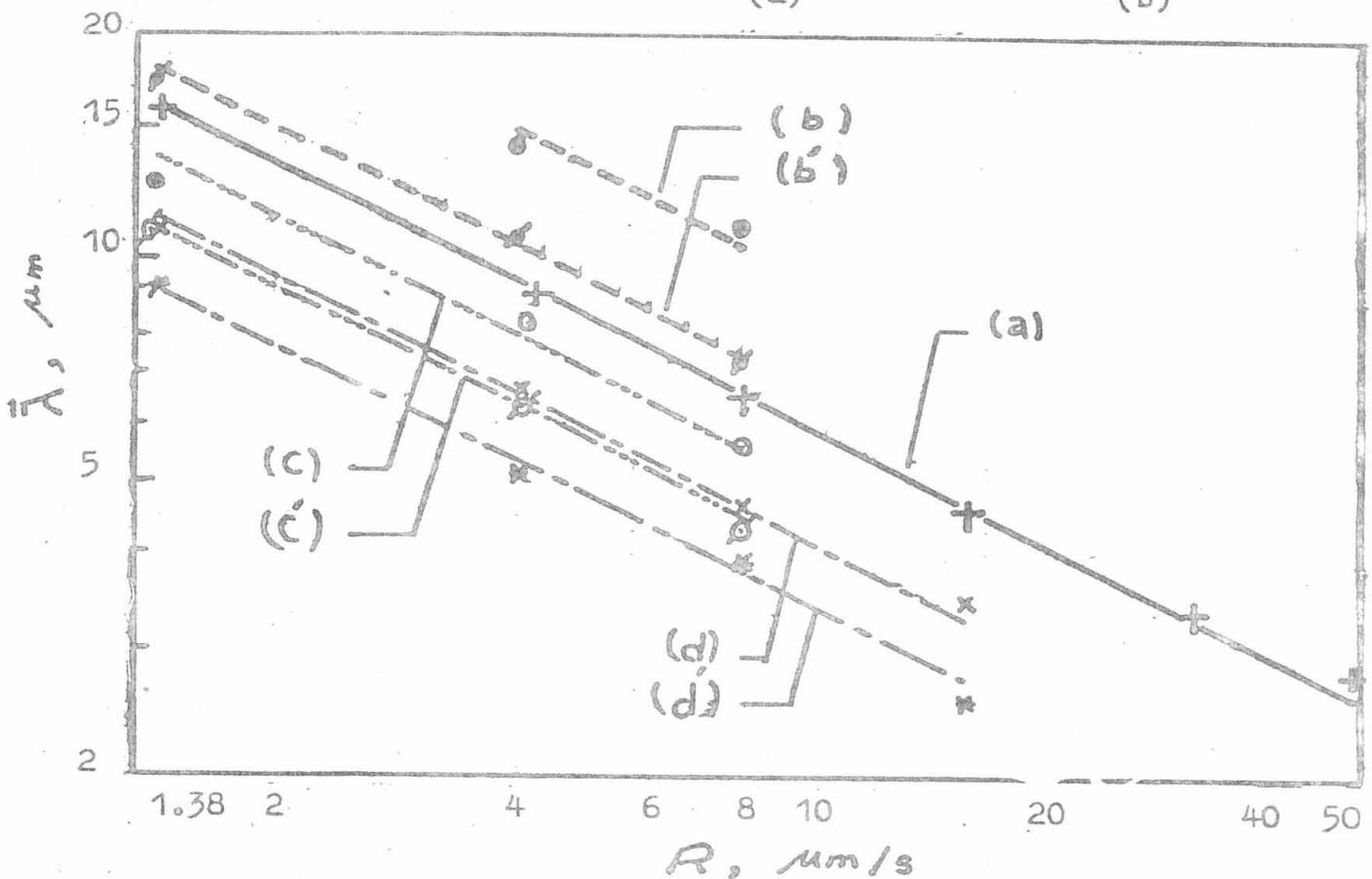
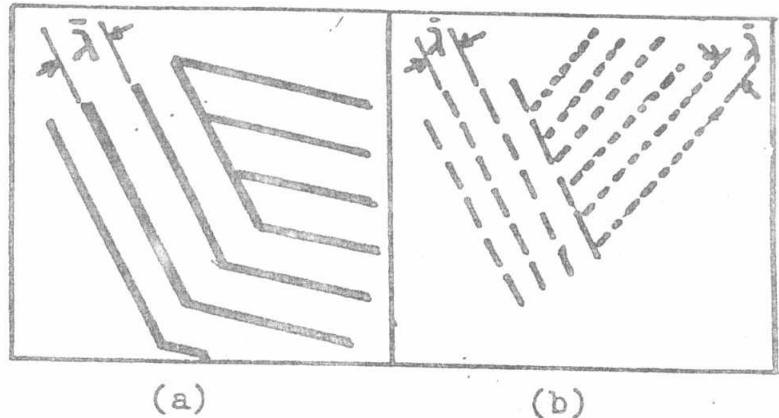


Fig.5:  $\bar{\lambda}$  as a function of R:

(a) pure eutectic composite,  
(b) with 0.3 wt% Al,  
(b) with 0.1 wt% Al,  
(c) with 0.1 wt% C,

(c) with 0.2 wt% C,  
(d) with 0.1 wt% Cr,  
(d) with 0.3 wt% Cr.



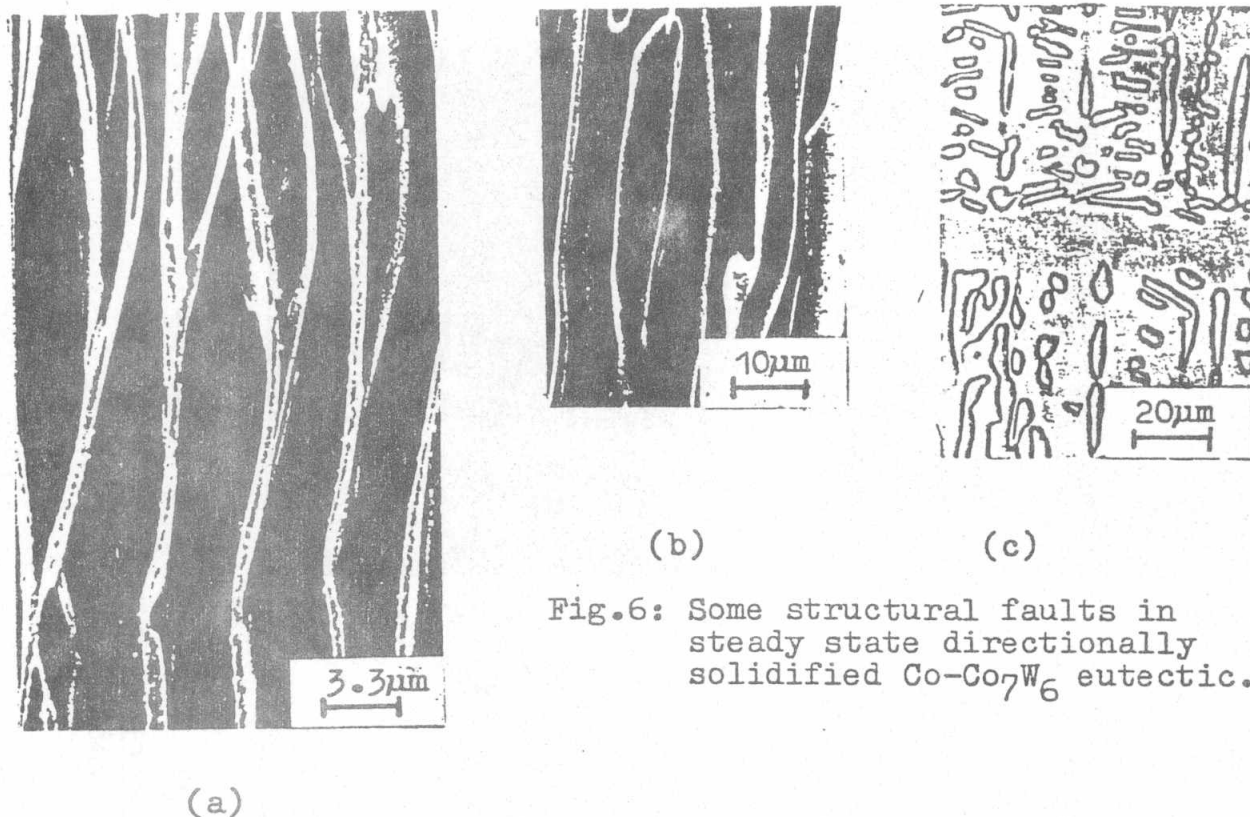


Fig.6: Some structural faults in steady state directionally solidified Co-Co<sub>7</sub>W<sub>6</sub> eutectic.

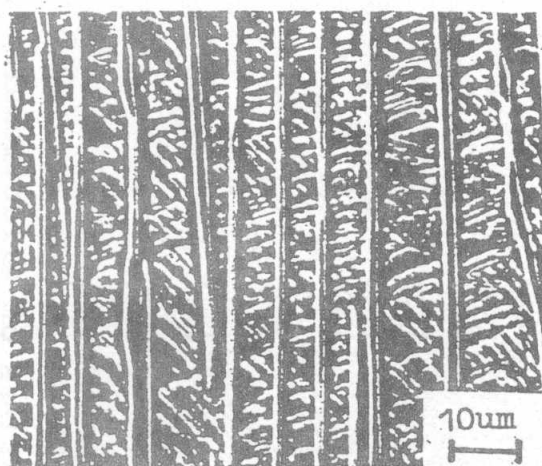
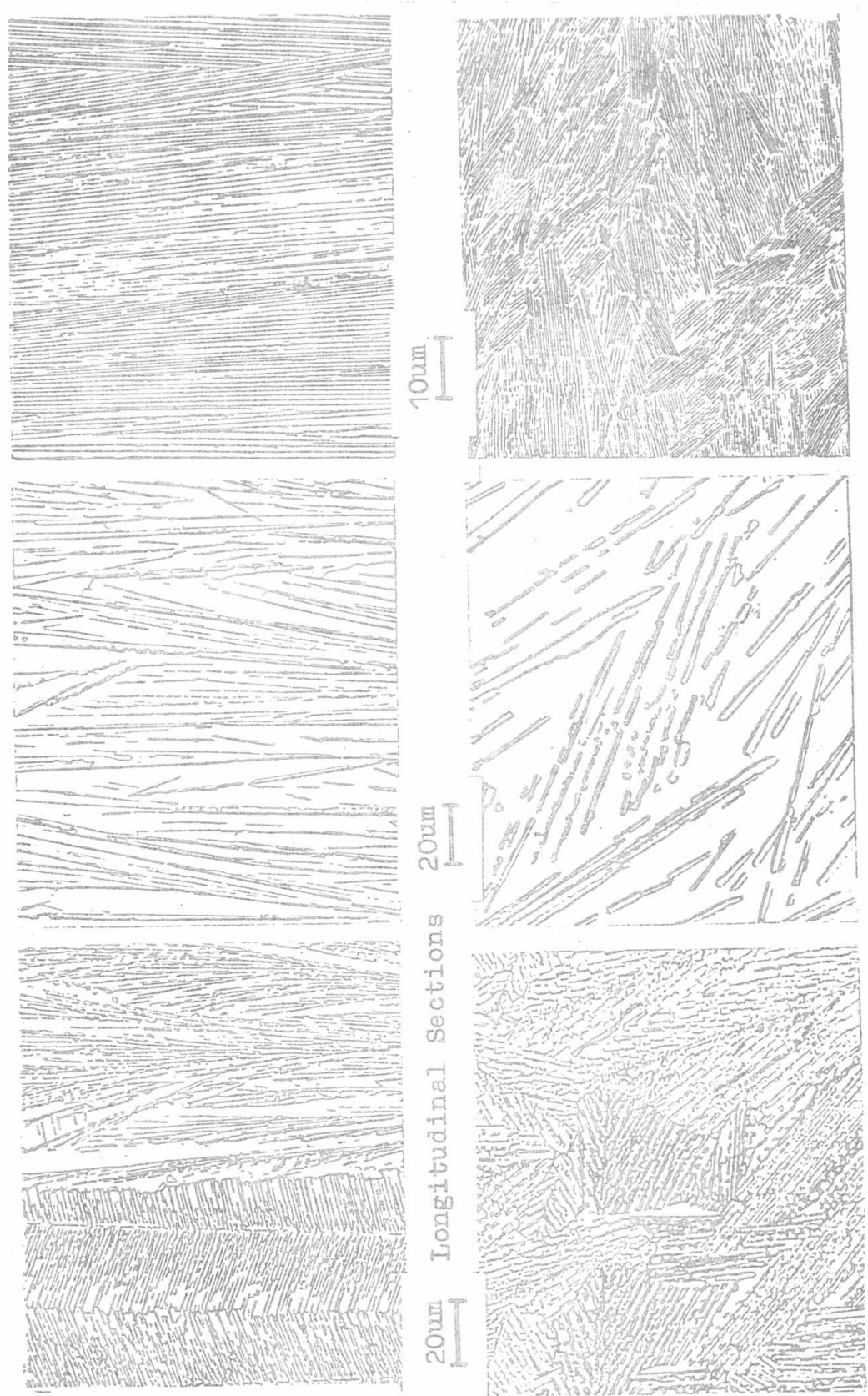


Fig.7: Peritectoid transformation observed between the Co<sub>7</sub>W<sub>6</sub> ribbons in a directionally solidified specimen, withdrawn below the peritectoid temperature, ( $R=4.3\mu\text{m/s}$ )

### Influence of Small Additions of Other Elements

The influence of small additions of some solute elements on the as-solidified structure has been also observed. The additions of C, Al and Cr as given in TABLE 1 have been considered. Generally the cellular morphology has been promoted and observed in specimens growing both at low and high  $R$ . The cells consists of either broken lamellae (or ribbons) in some grains of the specimens or the Co<sub>7</sub>W<sub>6</sub> phase with long side branches in other grains, Fig.8. Increasing  $R$  causes increase in the number of cells with the Co<sub>7</sub>W<sub>6</sub> phase with long side branches.



Longitudinal Sections      Transverse Sections

20μm      10μm

0.1 wt% Cr      0.3 wt% Al      0.1 wt% C

Fig.8: Structures of directionally solidified (R=4.3 um/s) Co-W eutectic with small solute additions

In the case of C additions, Fine particles are observed in the Co matrix which is beleived to be  $\gamma$  carbide(16,17) eutectic constituent. In the case of Cr additions, the shape of the structure has not been greatly influenced where perfect lamellae could be observed in some cells at low R. The influence of these additions on  $\bar{\lambda}$ , measured in the cell centre, is shown in Fig.5. In comparison with pure eutectic, it is clear that both C and Cr additions cause refining of the  $\text{Co}_7\text{W}_6$  phase and decrease in  $\bar{\lambda}$  values is resulted. The addition of Al, on the other hand causes coarsening and higher  $\bar{\lambda}$  values are resulted.

#### REFERENCES

1. Metals Handbook, published by ASM(1948)
2. M.W.Nevitt:Electronic structure and alloy chemistry,AIME symposium, Interscience publishers, New York (1963)p.101.
3. A.Moore and R.Elliott:J.Inst.Met.96(1978)p.62.
4. D.Jaffery and G.A.Chadwick:Trans.AIME 245(1969)p.2435.
5. S.Marich:J.Australian Inst. of Met.17(1972)p.18.
6. M.R.Taylor et al.:J.Cryst.Growth 3-4(1968)p.666.
7. P.J.Taylor et al.:Con.Met.Q.3(1964)p.235.
8. H.B.Smartt and T.H.Courtney:Met.Trans.3(1972)2000.
9. M.N.Croker et al.:J.Cryst.Growth 11(1971)p.121.
10. M.N.Croker et al.: ibid 30(1975)198
11. R.Elliott:Int.Met.Review-Review no. 219-(1977)p.161.
12. W.Kurz and P.R.Sahm:Gerichtet erstarrte Eutectische Werkstoffe, Springer Verlag, Berlin-Heidelberg-New York(1975).
13. R.S.Fidler, J.A.Spittle, M.R.Taylor and R.W.Smith: Solidification of Metals, ISI, (1968)p.173.
14. J.D.Hunt and D.T.J.Hurle: Trans.TMS-AIME 242(1968)p.1043.
15. R.T.Southin and B.L.Jones:J.Aust.Inst.Met.13(1968)p.203.
16. Richard L.Ashbrook and John .Wallace:Trans.AIME 236(1966) p.670.
17. P.Rautala and J.T.Norton:Trans.AIME 194(1956)p.1045.